

# Pressure dependence of limiting current density of sparking during electrochemical drilling

B. SAJDL

*J. Heyrovský Institute of Physical Chemistry, Academy of Sciences of the Czech Republic, 182 23 Prague 8, Czech Republic*

I. ROUŠAR

*Department of Inorganic Technology, University of Chemical Technology, 166 28 Prague 6, Czech Republic*

Received 31 March 1993; revised 19 November 1993

The cathodic current density used in electrochemical drilling can be increased only up to a certain value, above which current oscillations, sparking and acoustic phenomena appear, whereby the cathode can be damaged. The limiting current density for sparking,  $j_s$ , depends on the rate of flow and properties of the electrolyte and on the hydrostatic pressure. Values of  $j_s$  were measured for metal capillaries provided with external insulation in the turbulent flow regime in the range of Reynolds numbers from 2 300 up to 30 000 and at hydrostatic pressures ranging from 0.12 to 1.1 MPa. A simple heat generation model is proposed and the limiting current densities for sparking (868 experiments) are correlated with a criterion equation enabling the calculation of  $j_s$ .

## List of symbols

$c_{pE}$	specific heat of electrolyte ( $\text{J kg}^{-1} \text{K}^{-1}$ )
$d_1$	inner diameter of the cathode (m)
$d_2$	outer diameter of the cathode (m)
$I$	current (A)
$I_s$	limiting current for sparking (A)
$j$	current density ( $\text{A m}^{-2}$ )
$j_s$	limiting current density for sparking ( $\text{A m}^{-2}$ )
$K_T$	constant
$K_T^*$	constant
$L$	characteristic length (m)
$Nu$	Nusselt number
$p$	pressure (Pa)
$p_0$	reference atmospheric pressure (Pa)
$P$	exponent

$Pr$	Prandtl number
$q$	exponent
$\bar{q}$	heat flux ( $\text{W m}^{-2}$ )
$R$	exponent
$Re$	Reynolds number
$v_E$	linear electrolyte velocity ( $\text{m s}^{-1}$ )

## Greek symbols

$\alpha$	heat transfer coefficient ( $\text{W m}^{-2} \text{K}^{-1}$ )
$\theta$	temperature difference (K)
$\kappa_E$	electrolyte conductivity ( $\Omega^{-1} \text{m}^{-1}$ )
$\lambda_E$	electrolyte thermal conductivity ( $\text{W m}^{-1} \text{K}^{-1}$ )
$\mu_E$	electrolyte viscosity ( $\text{kg m}^{-1} \text{s}^{-1}$ )
$\rho_E$	electrolyte density ( $\text{kg m}^{-3}$ )

## 1. Introduction

Electrochemical machining (ECM) is based on controlled anodic dissolution of metals [1–9]. As a result of the initial nonuniform current distribution in the interelectrode gap filled with a streaming electrolyte, the shape of the cathode (tool) is copied into the anode (workpiece). The upper limit of practical current densities is limited by the removal of heat (to prevent boiling of the liquid) and reaction products (especially gas bubbles) from the interelectrode gap by the streaming electrolyte. If the cathodic current density is increased, other conditions being kept constant, electric discharges start to appear at a certain critical value,  $j_s$ .

Sparking during electrochemical machining was

studied also by Drake and McGeough [10] and McGeough and coworkers [11], who elaborated a very efficient method for drilling by simultaneous ECM and electrochemical arc machining (ECAM). They used an oscillating anode fed with pulsed direct current; the applied peak voltage was 25–55 V. They also studied the cathode tool wear during ECAM.

It is desirable to define the conditions under which sparking takes place, in order to attain the maximum velocity of machining without destabilizing the process or deteriorating the cathode. In practice, holes are drilled electrochemically with the use of a counter pressure of 1.0–1.6 MPa. Up to the present, the influence of pressure on the formation of discharges has not been elucidated. Therefore, the present work deals with the derivation of an equation for the calculation of

$j_s$  values applicable to electrochemical drilling of small holes, the external hydrostatic pressure being taken into account.

## 2. Influence of pressure on electric discharge

There is general agreement in the literature that the formation of a gas phase (by boiling, cavitation, or electrolysis) is the primary cause of the appearance of electric discharges in conducting liquids [12]. Since the main cathodic reaction product in ECM is hydrogen, increasing current density results in a lower electrical conductivity of the gas emulsion at the cathode and in a more intense heating of this region by the Joule heat. When the current density reaches the value of  $j_s$ , the cathode surface is covered by a continuous gas (vapour) layer formed by boiling liquid. Practically the entire voltage drop between the electrodes concentrates on this layer, which is subsequently broken through by an electric discharge accompanied by light and acoustic phenomena. According to another mechanism, the attainment of the critical current density,  $j_s$ , results in evaporation of the remaining electrolyte between gas bubbles and formation of an arc discharge, which is unstable and dies away. The described phenomena are periodically repeated.

Ebeid and coworkers [13] studied the influence of external conditions on the formation of discharges in electrochemical drilling. They found that practically no discharges occur below a certain threshold rate of machining and that the discharge can be suppressed by outer pressure; however, they did not indicate a quantitative correlation. Rumyantsev and Davydov [3] arrived at similar conclusions, supported by empirical findings from industrial practice. A model for calculation of the conditions of discharge formation without regard to the pressure was proposed in earlier work [14]. It is based on a general criterion equation describing the convective heat transfer in the near-cathode space. The equation was correlated with a set of experimental data and brought into a form enabling the calculation of  $j_s$  in electrochemical drilling for given cathode dimensions, rate of flow, and electrolyte composition.

It can be assumed that an increase of the outer hydrostatic pressure will result in a decrease of the bubble volume (volume fraction of gas in the gas emulsion) by compression and, to some extent, owing to higher solubility of the gas. Accordingly, the amount of heat evolved in the near-cathode space becomes lower. The dependence of  $j_s$  on pressure is significant. To determine this dependence and to verify it, the following procedure was chosen: (i) measurement of the dependence  $j_s$  on pressure under various conditions, (ii) derivation of an equation for this dependence and its correlation with experimental data.

A rigorous description of the heat transfer under the given conditions is extremely complicated. Therefore, the following general Dittus–Boelter criterion

equation for convective heat transfer in the turbulent region of electrolyte flow ( $Re \geq 2300$ ) [15] was used:

$$Nu = K_T Re^P Pr^{0.4} \left( \frac{d_1}{L} \right)^Q \quad (1)$$

Equation 1 was generalized for changing hydrostatic pressure to the form

$$Nu = K_T Re^P Pr^{0.4} \left( \frac{D_1}{L} \right)^Q \left( \frac{p}{p_0} \right)^R \quad (2)$$

Here,  $Nu$  denotes the Nusselt number defined as

$$Nu = \frac{\alpha L}{\lambda_E} \quad (3)$$

$Re$  denotes the Reynolds number

$$Re = \frac{v_E d_1 \rho_E}{\mu_E} \quad (4)$$

$Pr$  denotes the Prandtl number

$$Pr = \frac{c_{pE} \mu_E}{\lambda_E} \quad (5)$$

The characteristic dimension is defined as

$$L = \frac{d_2 - d_1}{2} \quad (6)$$

The geometrical ratio ( $d_1/L$ ) refers to the fact that the heat transfer and heat generation are concentrated at the capillary tip characterized by the dimensions  $L$  and  $d_1$ . It follows from Equations 1–4, that the heat transfer coefficient ( $\alpha$ ) at the tip of the metal capillary is influenced by the regime of electrolyte flow inside the capillary [14]. The Nusselt number for streaming of a liquid through a cylindrical tube considered here is given as

$$Nu = \frac{\bar{q} d_1}{\lambda_E \theta} \quad (7)$$

The heat flux density can be calculated as

$$q = \frac{j^2 L}{\kappa_E} \quad (8)$$

whence it is possible to express the current density  $j$ , which, in the limiting case of discharge formation, is equal to  $j_s$ :

$$j_s^2 = K_T \theta \frac{\kappa_E \lambda_E}{d_1 L} Re^P Pr^{0.4} \left( \frac{d_1}{L} \right)^Q \left( \frac{p}{p_0} \right)^R \quad (9)$$

The limiting current density for sparking,  $j_s$ , was calculated from the equation

$$j_s = \frac{4I_s}{\pi(d_2^2 - d_1^2)} \quad (10)$$

The portion of the current,  $I_s$ , flowing through the inner surface of the metal capillary can be neglected [16].

For the evaluation of the experiments, the substitution

$$K_T^* = K_T \theta \quad (11)$$

is made in Equation 9.

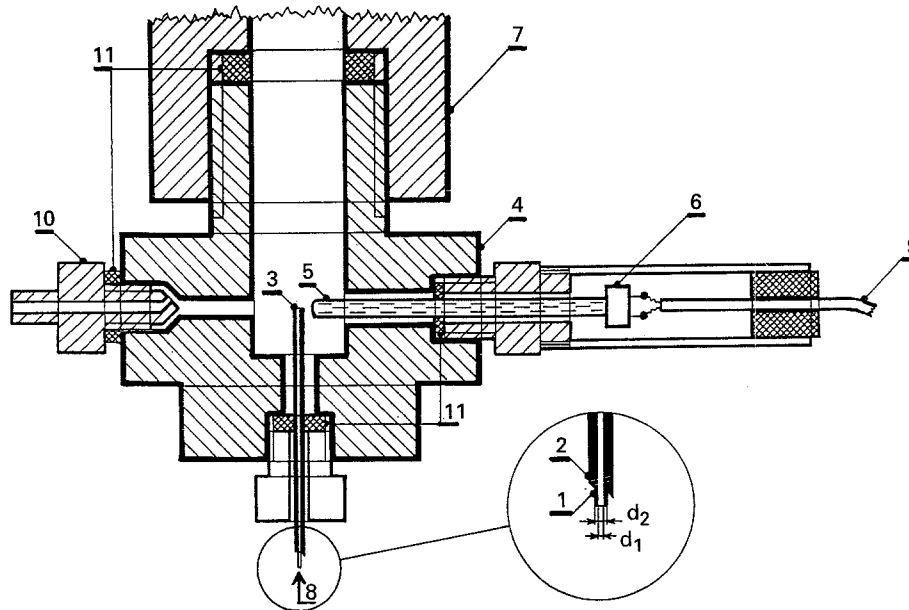


Fig. 1. Pressure cell. (1) Cathode (steel capillary), (2) insulation (ceramic), (3) working surface of cathode, (4) anode, (5) light-conducting quartz rod, (6) PIN diode, (7) flange of high-pressure air box, (8) electrolyte feed, (9) cable to optical power meter, (10) outlet valve, (11) gasket.  $d_1$  and  $d_2$  inner and outer diameter (without insulation) of cathode, respectively.

The aim of this work was the determination of the values of  $K_T^*$ ,  $P$ ,  $Q$  and  $R$  in Equation 9 from experimental data [17].

### 3. Experimental details

Holes of 1–3 mm diameter can be drilled electrochemically by using stainless steel capillaries, coated electrophoretically with a lacquer, enamel, or ceramic layer. Only the latter resisted the conditions prevailing during the formation of sparks. The pressure cell (Fig. 1) was made of mild steel and its inner surface functioned as anode. The cell was provided with a light-conducting quartz rod whose end was connected with a PIN diode for indication of the discharges. To maintain constant pressure, the cell was connected to an air box which was filled with nitrogen at the desired pressure before the experiment. The electrolyte was fed to the cathode through a high-pressure metering pump.

The properties of the electrolytes are given in Table 1, the inner diameters  $d_1$  of the cathodes were in the range from 0.53 mm to 1.07 mm, the outer diameters  $d_2$  of the cathodes were from 0.80 to 1.51 mm. The experimental conditions were consistent with those used in earlier work [14]. The measurements were

carried out at 20°C in the range of overpressures from 0 to 1 MPa. After the desired pressure and rate of flow of the electrolyte had been established, the d.c. voltage between the cathode and the anode was gradually raised until the optical power meter connected with the optical sensor showed a deflection. At that moment the value of the current  $I_s$  was recorded.

The construction of the apparatus permitted the cathode to be turned spatially by 180° to check whether the results were influenced by buoyancy acting on the gas bubbles, but no effect was found. The geometry of the cathode space is also unimportant [14]; experiments with a plate anode located at distances of 0.2 mm and 30–50 mm before the tip of the capillary showed that  $j_s$  does not depend on the distance between the anode and the cathode.

### 4. Results and discussion

In total 445 values of  $j_s$  were measured under various conditions for  $Re \in (2300; 30\,000)$  and hydrostatic pressure  $p \in (0.1, 1.1)$  MPa. These were supplemented by 423 values measured in a pressureless cell [18] in order to improve reliability of the calculated constants. For illustration, typical dependencies of

Table 1. Properties of electrolytes

Electrolyte	$\rho_E$ /kg m <sup>-3</sup>	$\mu_E \times 10^3$ /kg m <sup>-1</sup> s <sup>-1</sup>	$\kappa_E$ /Ω m <sup>-1</sup>	$\lambda_E$ /W m <sup>-1</sup> K <sup>-1</sup>	$c_{pE}$ /J kg <sup>-1</sup> K <sup>-1</sup>
25% NaCl	1191	1.81	21.4	0.572	2730
20% NaCl	1148	1.58	19.6	0.578	3060
15% NaCl	1109	1.28	16.4	0.584	3390
10% NaCl	1071	1.14	12.1	0.590	3720
5% NaCl	1034	1.09	6.7	0.594	4050
15% NaNO <sub>3</sub> + 20% NaClO <sub>3</sub>	1329	1.60	18.0	0.550	3400

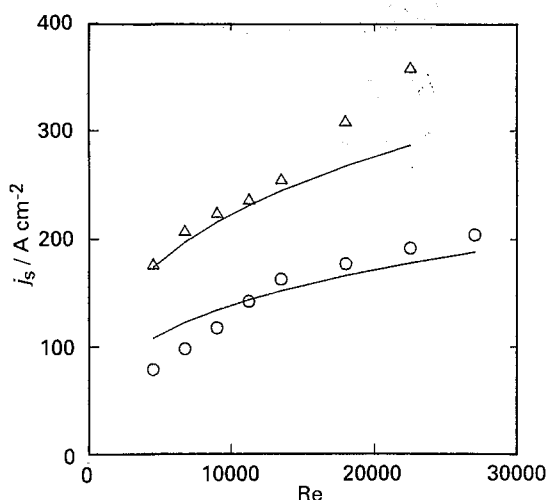


Fig. 2. Dependence of the limiting current density  $j_s$  on Reynolds number  $Re$  for pressures (○) 0.1 and (△) 1.1 MPa (a) and (b), and (—) the corresponding theoretical dependence (c); electrolyte 5% NaCl, inner diameter of the cathode 0.53 mm, outer diameter 1.20 mm.

the limiting current density on the Reynolds criterion are shown in Figs 2–4, corresponding to pressures 0.1 and 1.1 MPa. The whole set of 445 measured values of  $j_s$ , corresponding to overpressures of 0, 0.2, 0.5, and 1.0 MPa, Reynolds numbers in the range from 2300 to 30 000, and orientations of the cathode either upwards or downwards, was treated with the aim of optimizing the constants in Equation 9. The mean deviation between the measured and calculated  $j_s$  values served as a criterion for the correctness of Equation 9.

A comparison of the experimental values of  $j_s$  corresponding to  $p = p_0$  with those given in [18], based on visual observation of the sparks, revealed that the latter values are systematically lower. This is caused by the higher sensitivity of the eye compared with the sensor used. The ratio of  $j_s$  values found in the present work to those in [18] is approximately constant and was found by the least squares method to be 1.406.

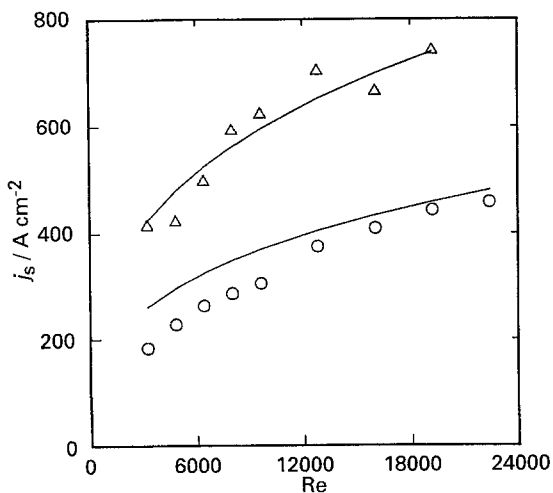


Fig. 3. Dependence of the limiting current density  $j_s$  on Reynolds number  $Re$  for pressures (○) 0.1 and (△) 1.1 MPa (a) and (b), and (—) the corresponding theoretical dependence (c); electrolyte 15% NaCl, inner diameter of the cathode 0.68 mm, outer diameter 1.01 mm.

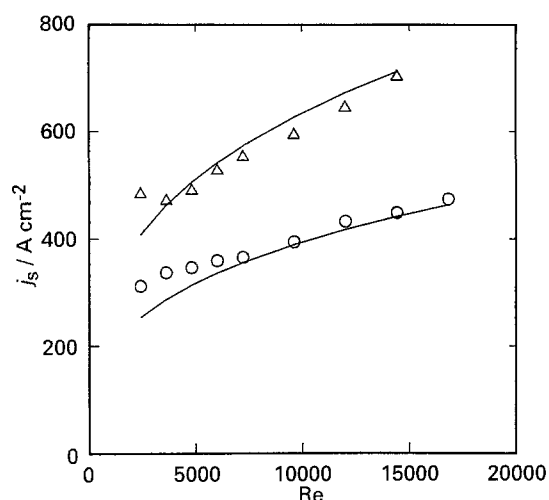


Fig. 4. Dependence of the limiting current density  $j_s$  on Reynolds number  $Re$  for pressures (○) 0.1 and (△) 1.1 MPa (a) and (b), and (—) the corresponding theoretical dependence (c); electrolyte 15% NaNO<sub>3</sub> + 20% NaClO<sub>3</sub>, inner diameter of the cathode 0.86 mm, outer diameter 1.19 mm.

Therefore, the  $j_s$  values in [18] were multiplied by this factor and included in the present work.

The constants in Equation 9 were determined by the least squares method as  $K_T^* = 92$ ,  $P = 0.62$ ,  $Q = 0.70$ ,  $R = 0.40$ . The relative standard deviation of all the measured  $j_s$  data from the calculated ones is 14.3%. A comparison of the measured  $j_s$  values with those calculated from the optimized Equation 9 can be seen from Figs 2–4.

In accord with the earlier findings [14, 16], the exponent of the Reynolds number is equal to 0.62. In contrast, the exponent  $Q$  of the ratio  $d_1/L$  is appreciably different; this is probably due to the relatively small range of this ratio used by the authors. The exponent for the pressure ratio,  $R = 0.40$ , represents well the expected influence of the pressure on the dimensions of gas bubbles in the emulsion near the cathode.

Similar experiments were carried out by Roušar and Riedel [19] in a flow-through channel with a small planar cathode located on its wall; the beginning of sparking was estimated visually. They found a higher exponent for the pressure term  $R = 0.7$ , but the upper limit for the Reynolds number was only 5900. This significant difference in the pressure exponent may be caused by the different geometry of the system and perhaps by a different way of estimation of the beginning of sparking.

Equation 9 can be used for prediction of  $j_s$  in technical practice, where a higher pressure is used.

## References

- [1] V. A. Gusef, *British Patent 335 003* (1930).
- [2] J. A. McGeough, 'Principles of Electrochemical Machining', Chapman & Hall, London (1974).
- [3] E. M. Rummyantsev and A. D. Davydov, 'Tekhnologiya elektrokhimicheskoy obrabotki metallov', Vysshaiya shkola, Moscow (1984).
- [4] J. F. Wilson, 'Practice and Theory of Electrochemical Machining', Wiley Interscience, New York (1971).
- [5] R. A. Mirzoev, 'Cathode Process during ECM', Collected papers on ECM, Schtiinca, Kischinev (1971) (in Russian).

- [6] A. D. Davydov, V. D. Kashtchev and B. N. Kabanov, *Elektron. Obrab. Mater.* No. 6, (1969) 13.
- [7] M. Datta and D. Landolt, *Electrochim. Acta* **26** (1981) 899.
- [8] *Idem, ibid.* **27** (1982) 385.
- [9] D. Landolt, R. Acosta, R. H. Müller and C. W. Tobias, *J. Electrochem. Soc.* **117** (1970) 839.
- [10] T. H. Drake and J. A. McGeough, *Proceedings of Machine Tool Design and Research Conference*, Manchester, Macmillan (1981) p. 361.
- [11] I. M. Crichton, J. A. McGeough, E. Munro and C. White, *Precision Engineering*, July (1981), (cited in [10]).
- [12] P. P. Maljushevskii, G. G. Gorovenko, S. G. Poklonov, V. I. Levda, L. P. Trofimova, N. I. Kuskova, Yu. G. Golubenko and Z. K. Krivitskaya, *Elektron. Obrab. Mater.* **136** (1987) 33.
- [13] S. J. Ebeid, E. M. Baxter and C. N. Larsson, *Proceedings of the 19th International Machine Tool Design and Research Conference*, University of Manchester, Manchester (1979).
- [14] P. Novák, B. Sajdl and I. Roušar, *Electrochim. Acta* **30** (1985) 43.
- [15] E. R. G. Eckert, 'Heat and Mass Transfer', McGraw-Hill Book Company, New York (1959).
- [16] P. Novák, I. Roušar, A. Kimla, V. Mejta and V. Cezner, *Coll. Czech. Chem. Commun.* **46** (1981) 2949.
- [17] B. Sajdl, PhD thesis, (in Czech), University of Chemical Technology, Prague (1993).
- [18] P. Novák, PhD thesis, (in Czech), University of Chemical Technology, Prague (1982).
- [19] I. Roušar and T. Riedel, *J. Appl. Electrochem.*, in press.